


Multiparametric Quantitative Brain MRI in Neurological and Hepatic Forms of Wilson's Disease

Monika Dezortova, PhD,¹ Artem Lescinskij, MD,^{1,2} Petr Dusek, MD, PhD,^{2,3*} 
Vit Herynek, PhD,^{1,4} Julio Acosta-Cabronero, PhD,⁵ Radan Bruha, MD, PhD,⁶ Filip Jiru, PhD,¹
Simon D. Robinson, PhD,⁷ and Milan Hajek, PhD¹

Background: In Wilson's disease (WD), demyelination, rarefaction, gliosis, and iron accumulation in the deep gray matter cause opposing effects on T_2 -weighted MR signal. However, the degree and interplay of these changes in chronically treated WD patients has not been quantitatively studied.

Purpose: To compare differences in brain multiparametric mapping between controls and chronically treated WD patients with neurological (neuro-WD) and hepatic (hep-WD) forms to infer the nature of residual WD neuropathology.

Study Type: Cross-sectional.

Population/Subjects: Thirty-eight WD patients (28 neuro-WD, 10 hep-WD); 26 healthy controls.

Field Strength/Sequence: 3.0T: susceptibility, T_2^* , T_2 , T_1 relaxometry; 1.5T: T_2 , T_1 relaxometry.

Assessment: The following 3D regions of interest (ROIs) were manually segmented: globus pallidus, putamen, caudate nucleus, and thalamus. Mean bulk magnetic susceptibility, T_2^* , T_2 , and T_1 relaxation times were calculated for each ROI.

Statistical Tests: The effect of group (neuro-WD, hep-WD, controls) and age was assessed using a generalized least squares model with different variance for each ROI and quantitative parameter. A general linear hypothesis test with Tukey adjustment was used for post-hoc between-group analysis; $P < 0.05$ was considered significant.

Results: Susceptibility values were higher in all ROIs in neuro-WD compared to controls and hep-WD ($P < 0.001$). In basal ganglia, lower T_2 and T_2^* were found in neuro-WD compared to controls ($P < 0.01$) and hep-WD ($P < 0.05$) at 3.0T. Much smaller intergroup differences for T_2 in basal ganglia were observed at 1.5T compared to 3.0T. In the thalamus, increased susceptibility in neuro-WD was accompanied by increased T_1 at both field strengths ($P < 0.001$ to both groups), and an increased T_2 at 1.5T only ($P < 0.001$ to both groups).

Data Conclusion: We observed significant residual brain MRI abnormalities in neuro-WD but not in hep-WD patients on chronic anticopper treatment. Patterns of changes were suggestive of iron accumulation in the basal ganglia and demyelination in the thalamus; 3.0T was more sensitive for detection of the former and 1.5T of the latter abnormality.

Level of Evidence: 2

Technical Efficacy Stage: 3

J. MAGN. RESON. IMAGING 2019.

WILSON'S DISEASE (WD) is an autosomal recessive disorder caused by mutation of the *ATP7B* gene, characterized by disturbances in copper metabolism which lead to gradual accumulation of the metal in body organs.¹ The *ATP7B* protein is mainly expressed in hepatocytes, while copper is primarily deposited in the liver, causing hepatic

View this article online at wileyonlinelibrary.com. DOI: 10.1002/jmri.26984

Received Aug 7, 2019, Accepted for publication Oct 17, 2019.

*Address reprint requests to: P.D., Department of Neurology, 1st Faculty of Medicine and General University Hospital in Prague, Katerinska 30, 120 00, Praha 2, Czech Republic. E-mail: petr.dusek@vfn.cz

Contract grant sponsor: Ministry of Health of the Czech Republic; Contract grant number: AZV 15-25602A; Contract grant sponsor: DRO Institute for Clinical and Experimental Medicine – IKEM, IN 00023001.

From the ¹MR Unit, Department of Diagnostic and Interventional Radiology, Institute for Clinical and Experimental Medicine, Prague, Czech Republic; ²Department of Radiology, First Faculty of Medicine, Charles University and General University Hospital, Prague, Czech Republic; ³Department of Neurology and Centre of Clinical Neuroscience, First Faculty of Medicine, Charles University and General University Hospital, Prague, Czech Republic; ⁴Center for Advanced Preclinical Imaging, First Faculty of Medicine, Charles University, Prague, Czech Republic; ⁵Tenoke Ltd, Cambridge, UK; ⁶Fourth Department of Internal Medicine, First Faculty of Medicine, Charles University and General University Hospital, Prague, Czech Republic; and ⁷High Field MR Centre, Department of Biomedical Imaging and Image-guided Therapy, Medical University of Vienna, Vienna, Austria

symptoms; this stage is referred to as the hepatic form of WD (hep-WD).¹ In later stages of the disease, copper accumulates in other organs, mainly in the brain, leading to a neurological form of WD (neuro-WD) manifesting in neurological and psychiatric symptoms.¹

Abnormal findings on brain magnetic resonance imaging (MRI) are present in more than 90% of neuro-WD and ~40–70% of hep-WD patients.^{2,3} The most prominent findings in untreated patients are symmetrically increased T_2 signals in deep gray matter (DGM) nuclei and mesencephalic and pontine white matter. These T_2 hyperintense lesions, which presumably reflect edema and demyelination caused by copper toxicity, are partly reversible with anticopper treatment.^{4,5} In cases of more severe tissue damage, increased T_2 signals may indicate astrogliosis, tissue rarefaction, or even cavitation, which are irreversible and persist despite long-term anticopper treatment.⁶

Along with these T_2 hyperintense lesions, T_2 signals from DGM in neuro-WD patients may be influenced by the accumulation of iron species, inducing T_2 hypointensities.⁷ An association between increased R_2^* values (ie, relaxivity, the reciprocal value of T_2^*) and iron concentrations in the basal ganglia of WD brains has been confirmed by postmortem MRI histopathology correlation.⁸ Increased deposition of paramagnetic compounds in DGM in neuro-WD patients has also been consistently reported in previous in vivo studies utilizing quantitative susceptibility mapping (QSM) and R_2^* relaxometry.^{9,10} Notably, in contrast to T_2 hyperintensities, which gradually diminish, T_2 hypointensities in DGM may progress despite anticopper treatment.¹⁰ Described pathologies, which have opposing effects on T_2 relaxation time, typically coexist in the DGM of WD patients. We hypothesized that this interplay between factors, which have the effect of either increasing (eg, demyelination, astrogliosis, or tissue rarefaction) or decreasing (eg, iron accumulation) T_2 -weighted signals, would also be sensitive to different magnetic field strengths. Specifically, imaging at higher magnetic fields enhances sensitivity to the effect of paramagnetic compounds, thus increasing the prominence of hypointense lesions and potentially overshadowing T_2 hyperintensities. It has been suggested that changes in T_2 relaxation time measured at two or more magnetic fields—also known as field-dependent relaxivity increase (FDRI)—are a sensitive measure of paramagnetic tissue content, supposedly driven by ferritin concentration.^{11,12} Surprisingly, there is a paucity of quantitative brain MRI studies on WD and, to our knowledge, no study has compared relaxometry at different magnetic fields.

The aims of this study were as follows: 1) to compare differences in multiparametric mapping (bulk magnetic susceptibility, T_2^* , T_2 , T_1) between controls and chronically treated WD patients with neurological and hepatic forms; 2) to infer the nature of the residual WD neuropathology; and 3) to examine differences between T_2 and T_1 relaxometry at 1.5T and 3T magnetic fields.

Materials and Methods

Subjects

We prospectively investigated 38 patients with genetically confirmed WD on a stable anticopper treatment (28 with neuro-WD: 13f/15m, mean age 47.1 ± 9.5 [28.2–64.2] years; 10 with mild hep-WD: 5f/5m, mean age 33.8 ± 10.9 [19.1–52.2] years); and 26 healthy volunteers (14f/12m, 44.8 ± 11.7 [24.0–68.4] years). All subjects underwent MR examinations at 1.5T and 3T, serum ceruloplasmin oxidase activity test, and neurologic examination. All subjects were informed about the study and signed a written consent in agreement with Ethical Committee rules.

Neuro-WD was defined as the presence of neurologic symptoms typical for WD at the onset or any time during the course (due to undertreatment) of the disease. Mean treatment duration for the neuro-WD group was 17.6 ± 12.6 (2–46) years; 13 patients were on D-penicillamine, 5 on zinc-sulfate, and 10 were on a combined therapy D-penicillamine + zinc-sulfate.

Hep-WD was defined as the absence of neurologic symptoms during the disease course. Mean treatment duration for the hep-WD group was 20.9 ± 11.4 (3–42) years; seven patients were on D-penicillamine, two on zinc-sulfate, and one was on a combined D-penicillamine and zinc-sulfate therapy. Severe or decompensated liver cirrhosis as well as clinical signs of hepatic encephalopathy were exclusion criteria for both WD groups. The group of hep-WD patients who agreed to take part in our study was younger compared to neuro-WD and controls ($P < 0.01$).

Controls were recruited from coworkers and their friends and families; they were selected to be age- and sex-matched to neuro-WD patients. Subjects with a history of neurological or psychiatric problems were excluded. Serum ceruloplasmin oxidase activity was normal in all control subjects.

MRI

For MRI, 1.5T (Avanto Fit) and 3T (Trio) MR scanners (Siemens Healthineers, Erlangen, Germany) with 12-channel birdcage head coils were used. A standard clinical examination with the 3T MRI protocol was supplemented by QSM, T_2^* , T_1 , and T_2 relaxometry. The 1.5T system was used for measurement of T_1 and T_2 relaxometry values, employing the same voxel resolution and slice positioning as the 3T system.

Susceptibility Mapping

QSM and T_2^* relaxometry maps were reconstructed from a 3D multi-echo gradient recalled echo (GRE) sequence (repetition time [TR] = 40 msec; six equidistant echo times [TEs] between 5.22 and 34.64 msec; flip angle [FA] = 15° ; voxel resolution = $0.8 \times 0.8 \times 2$ mm³; BW = 450 Hz/pixel). Phase images were reconstructed offline using a virtual reference coil approach.¹³ The QSM reconstruction pipeline was largely analogous to that used in a previous Parkinson's disease study¹⁴; the present implementation consisted of: 1) continuous Laplacian-based phase unwrapping¹⁵; 2) variable, spherical mean value property-based background field removal¹⁶ using a 10 mm starting kernel radius; and 3) nonlinear morphology-enabled dipole inversion (nMEDI) with $\lambda = 1000$.¹⁷ Mean bulk magnetic susceptibility values were calculated using the following 3D ROIs (manually traced by a single rater [A.L., 3 years of experience] using ITK-SNAP software [www.itksnap.org]):

globus pallidus (GP), putamen (Put), caudate nucleus (CN), and thalamus (Th). Magnetic susceptibility values were normalized by subtracting the value measured in the occipital white matter reference region.

Relaxometry

Carr–Purcell–Meiboom–Gill sequences (TR = 3000 msec; 32 echoes with TE step 8.3 msec at 3T and 6.9 msec at 1.5T, FA = 180°; voxel size $0.8 \times 0.8 \times 5 \text{ mm}^3$) were used to calculate T_2 relaxation time maps. T_1 relaxation time maps for the same slices were measured using inversion recovery procedure with 10 inversion time values TI (250–4000 msec) at 3T and 9 TI values (300–4000 msec) at 1.5T; the images were acquired by a steady-state gradient echo sequence (FISP, 3T: TR/TE = 5000/1.49 msec, FA = 35°; 1.5T: TR/TE = 5000/1.51 msec; FA = 35°). Relaxation maps were calculated using the in-house-developed VIDI program¹⁸ and GP, Put, CN, and Th regional T_1 and T_2 values were averaged for the left and right hemispheres. Two raters (A.L.; V.H. 20 years of experience) performed manual segmentation of T_1 and T_2 maps, each of them segmented data from approximately half of the subjects (both patients and controls). Correlation analysis of mean ROI values obtained by both raters was done on a subgroup of eight subjects confirming high between-rater agreement for T_2 ($r = 0.949$, $P < 0.0001$) and T_1 ($r = 0.946$, $P < 0.0001$) relaxation times. T_2 relaxation time dependence on the magnetic field was expressed by a slope S of R_2 relaxivity calculated according to a formula:

$$S = \left(1/T_2^{(3T)} - 1/T_2^{(1.5T)} \right) / \Delta B \left[s^{-1} T^{-1} \right]$$

where ΔB is a difference in magnetic fields.

T_2^* values were calculated from multiecho GRE magnitude images using nonlinear least-squares fitting according to the Levenberg–Marquardt algorithm (MRI Processor v. 1.1.6, ImageJ 1.51k, NIH; T_2^* values were capped at 100 msec, the maximum number of iterations was 100, and forced no bias).¹⁹ The 3D ROIs used for magnetic susceptibility analysis were also applied to the T_2^* maps, retrieving mean bulk values for each region.

Statistical Analysis

Data were analyzed using R software.²⁰ A generalized least-squares model with different variance for each group:

$$Y_{ij} = Age_{ij} + GROUP_j + \varepsilon_{ij}; \varepsilon_{ij} \sim N(0, \sigma^2)$$

was used for each ROI and quantitative parameter to correct for physiological brain iron accumulation with normal aging and unequal variances of the groups. The Bonferroni procedure was used to correct for multiple comparisons; $P < 0.0125$ was considered significant. Distribution of model residuals was visually evaluated using a Q-Q plot. In the case of apparent nonnormal distribution, the dependent variable was logarithmically transformed, or the most prominent outliers were excluded. The general linear hypothesis test with Tukey adjustment was used for post-hoc between-group analysis; $P < 0.05$ was considered significant.

Results

Susceptibility values were significantly higher for all examined structures (GP, Put, CN, Th) in neuro-WD patients compared to controls ($P < 0.001$) and hep-WD patients ($P < 0.001$). The most pronounced difference was observed in the putamen, where the susceptibility increase was more than 100% ($P < 0.001$, 95% confidence interval [CI] 1.7–2.8; Table 1, Fig. 1). Susceptibility in the putamen also showed a significant effect of age ($P < 0.001$). Point estimates of susceptibility were systematically slightly higher in the hep-WD group compared to controls, except for the putamen, but the difference was not statistically significant.

T_2 and T_2^* relaxation times at 3T were significantly shorter in the neuro-WD group compared to controls for all DGM structures, except for the thalamus ($P < 0.01$). Significant differences between neuro-WD and hep-WD were found in GP and Put ($P < 0.05$) for T_2 and in Put, CN, and GP for T_2^* relaxation times ($P < 0.01$). T_2 and T_2^* relaxation times in hep-WD did not differ from controls in any of the examined regions. Significant effect of age was found in CN for T_1 and T_2 , as well as T_2^* relaxation times ($P < 0.01$) and in Th and Put for T_2 and T_2^* relaxation times ($P < 0.01$) at 3T. Contrary to T_2 or T_2^* , T_1 relaxometry revealed differences only in the thalamus, with the neuro-WD group showing significantly longer T_1 relaxation times compared to controls ($P < 0.001$, 95% CI 64.7–126.2) and hep-WD patients ($P < 0.001$, 95% CI 43.9–128.8).

In CN, and GP, 1.5T results followed the same pattern as observed for 3T data except for an insignificant difference between hep-WD and neuro-WD for T_2 in the GP ($P = 0.29$, 95% CI -4.9 – 1.1); no difference between groups was found in Put ($P = 0.064$) (Table 2). Interestingly, differences in the thalamus in the neuro-WD group were more pronounced at lower magnetic field strength (ie, 1.5T). In particular, significantly longer T_2 and T_1 relaxation times were observed in the neuro-WD compared to healthy and hep-WD groups ($P < 0.001$).

Field-dependent changes in R_2 relaxivity values were calculated from data acquired at 1.5T and 3T. Slopes of R_2 field dependence were significantly steeper in the neuro-WD group in comparison to controls in all examined regions ($P < 0.01$) and in Put and Th compared to hep-WD patients ($P < 0.01$). No significant differences were found between the hep-WD and control groups (Table 3). A significant effect of age was observed in NC and Put ($P < 0.01$).

Discussion

We applied quantitative MR methods at two magnetic field strengths to determine neuroimaging alterations in patients with hepatic and neurological forms of WD on long-term anticopper treatment, comparing them with healthy controls to explore the nature of the residual brain tissue pathology.

In the neuro-WD group we found significantly increased magnetic susceptibility values in all DGM nuclei

TABLE 1. T_2^* , T_2 , and T_1 Relaxation Times (msec) and Susceptibility (ppb) Values at 3T in the Basal Ganglia (Globus Pallidus [GP], Putamen [Put], and Caudate Nucleus [CN]) and Thalamus (Th)

Susceptibility	GP	Put	CN	Th
Neuro-WD	159.7 (33.4)	100.4 (37.7)	83.0 (21.0)	24.0 (7.8)
Hep-WD	111.7 (21.9)***	38.3 (15.5)***	52.3 (10.3)***	11.6 (4.0)***
Controls	101.0 (11.5)***	46.6 (19.8)***	50.4 (12.8)***	9.5 (4.4)***
T_2^*	GP	Put	CN	Th
Neuro-WD	22.34 (3.8)	31.1 (6.5)	38.24 (7.1)	49.10 (5.6)
Hep-WD	27.74 (3.4)**	42.76 (6.2)***	48.75 (4.9)***	49.72 (3.1)
Controls	28.67 (2.4)***	40.67 (5.4)***	48.99 (4.5)***	51.58 (2.8)
T_2	GP	Put	CN	Th
Neuro-WD	54.9 (4.9)	64.8 (6.2)	72.7 (5.1)	77.3 (3.5)
Hep-WD	58.3 (3.8)*	70.6 (5.2)*	77.3 (5.9)	75.5 (2.6)
Controls	59.6 (2.6)***	69.1 (3.6)**	78.0 (2.7)***	76.6 (2.1)
T_1	GP	Put	CN	Th
Neuro-WD	1048.8 (85.6)	1216.4 (84.4)	1330.9 (106.3)	1235.0 (53.7)
Hep-WD	1030.2 (51.5)	1232.5 (53.2)	1352.0 (51.9)	1152.8 (43.3)***
Controls	1028.4 (43.7)	1210.6 (43.8)	1342.8 (32.6)	1140.4 (38.4)***

Standard deviations are in parentheses.

* $P < 0.05$.

** $P < 0.01$, and.

*** $P < 0.001$ for the post-hoc between-group analysis of control and hep-WD vs. neuro-WD group.

and decreased T_2 and T_2^* relaxation times in the GP, Put, and CN at 3T as compared to the hep-WD and control groups. We also observed increased T_1 and T_2 relaxation times in the thalamus in neuro-WD group, but the latter was only significant with data acquired at 1.5T.

The pattern of changes found in the basal ganglia of neuro-WD patients, namely, increased bulk magnetic susceptibility, decreased T_2 (particularly at 3T) and T_2^* relaxation times, and steeper FDRI slopes, is consistent with stronger paramagnetic behavior in these structures. The most affected area was the putamen, with a more than 100% increase in magnetic susceptibility in the neuro-WD group compared to controls. We attribute the changes in susceptibility and T_2^* relaxation times to increased iron content since postmortem studies show that R_2^* relaxometry values closely correlate with iron content, but not with copper concentrations in the basal ganglia of WD patients.^{8,21} It should be noted that Cu^{2+} species are paramagnetic, and we cannot exclude that they could have some impact on quantitative measurements. However, copper concentration in DGM is approximately three times lower than iron concentration even in neuro-WD patients⁸ and although

magnetic properties of copper storage compounds in WD are not exactly known, susceptibility of $\text{Fe}^{2+/3+}$ species is typically higher than susceptibility of Cu^{2+} species. Based on these facts, we assume that the copper contribution to susceptibility and relaxometry measurements in DGM is rather small.

It has long been acknowledged that gradual accumulation of iron in the basal ganglia is a natural process of aging.²² Most non-hemin iron in the brain is stored in a pool consisting of either ferritin or hemosiderin. Earlier studies have shown that, if an increased iron content is not accompanied by a reduction in T_1 , it could indicate a deposition of an insoluble paramagnetic compound. It is contrary to ferritin, which is known to affect both T_1 and T_2 relaxations.^{23,24} We assume, thus, that excess iron in neuro-WD might be in a form of hemosiderin, which has a strong impact on T_2 , T_2^* , and susceptibility, but a negligible influence on T_1 due to its insolubility.

Interestingly, we observed a different pattern in the thalamus of neuro-WD patients, ie, increased magnetic susceptibility and T_2 relaxation times at 1.5T and unaltered T_2^* and T_2 relaxation times at 3T. This points to a decrease in tissue diamagnetism, possibly due to a loss of myelin, as opposed to an

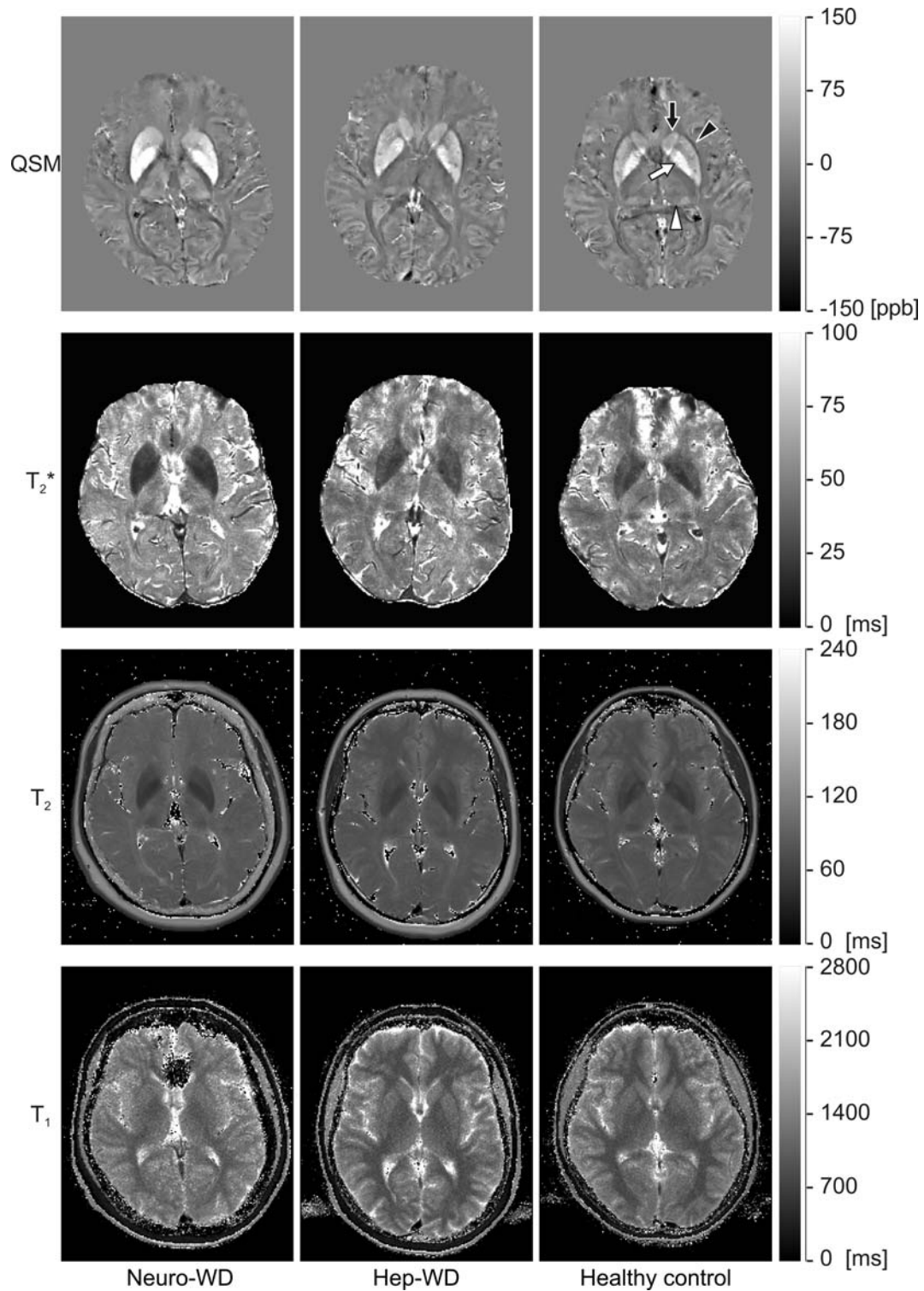


FIGURE 1: QSM images (scale in ppb) and T_2^* , T_2 , and T_1 relaxation maps (scale in msec) acquired at 3T of illustrative neuro-WD (left), hep-WD (middle), and healthy control (right) subjects, with greater magnetic susceptibility and shorter T_2 and T_2^* relaxation times visible in the basal ganglia of the neuro-WD patient. Note also greater magnetic susceptibility in the thalamus of the neuro-WD case. Black arrow: caudate nucleus; black arrowhead: putamen, white arrow: globus pallidus; white arrowhead: thalamus.

accumulation of paramagnetic compounds. A longer T_1 relaxation time is also attributed to lipid loss and/or increased tissue water content. Taken together, our findings are consistent with demyelination of the thalamus in neuro-WD patients. Previous

diffusion tensor imaging (DTI) studies have identified abnormalities in the thalami of WD patients, specifically increased mean diffusivity and decreased fractional anisotropy, which may be theoretically driven by demyelination processes.²⁵

TABLE 2. T₂ and T₁ Relaxation Times (msec) at 1.5T in the Basal Ganglia (Globus Pallidus [GP], Putamen [Put], and Caudate Nucleus [CN]) and Thalamus (Th)

T2	GP	Put	CN	Th
Neuro-WD	65.6 (4.3)	75.2 (3.8)	83.0 (3.9)	82.3 (3.3)
Hep-WD	66.9 (2.7)	78.1 (3.7)	85.9 (3.9)*	78.0 (2.4)***
Controls	68.2 (1.8)**	77.4 (2.2)	85.9 (1.9)**	78.7 (1.7)***
T1	GP	Put	CN	Th
Neuro-WD	795.4 (79.0)	958.3 (69.2)	1054.2 (64.6)	942.0 (47.2)
Hep-WD	769.8 (34.1)	968.3 (43.2)	1076.4 (41.4)	861.1 (37.0)***
Controls	779.4 (37.3)	962.1 (28.0)	1059.4 (24.8)	857.8 (32.8)***

Standard deviations are in parentheses.

* $P < 0.05$.

** $P < 0.01$, and.

*** $P < 0.001$ for the post-hoc between-group analysis of control and hep-WD vs. neuro-WD group.

Total R_2 and R_2^* relaxivities are the sum of all paramagnetic (ie, iron-driven) and diamagnetic (ie, myelin-driven) contributions. At higher magnetic fields (3T vs. 1.5T), the paramagnetic contribution to transverse relaxivity increases, but the diamagnetic contribution remains approximately the same. This causes a decrease of the T_2 or T_2^* -weighted signal intensity of iron-containing tissues at 3T, unlike in 1.5T MR images. Notably, the majority of early neuroimaging studies in WD were performed at low magnetic field strengths (ie, ≤ 1.5 T), which explains the relative prominence of T_2 hyperintense lesions in comparison to T_2 hypointensities in DGM in these studies.²⁶

Accordingly, in the present study between-group differences of T_2 values in the basal ganglia were more pronounced at the 3T magnetic field strength (eg, in GP: 8.8% at 3T and 4.1% at 1.5T; Tables 1 and 2). This finding confirms that abnormal T_2 relaxation time values in the basal ganglia of chronically treated neuro-WD patients are predominantly driven by iron deposition. The opposite effect was observed in the

thalamus, where significantly increased T_2 values in neuro-WD patients were only found on data acquired at 1.5T but not at 3T. This observation suggests that other factors less sensitive to magnetic field strength, ie, demyelination and/or increased tissue water content, are primary factors contributing to abnormal T_2 values in the thalamus. We presume that higher sensitivity to paramagnetic contribution mitigates this effect at 3T magnetic field strength.

R_2 relaxivity slopes were steeper for all analyzed regions in neuro-WD patients compared to controls, which is compatible with higher concentration of paramagnetic compounds in the former group. For GP, putamen, and caudate, the observed differences were comparable to the analysis of T_2 values at 3T. This is in line with a recent study showing that calculation of R_2 relaxivity slopes from measurements at two magnetic fields bring no benefit compared to measurement of R_2 relaxometry at the higher magnetic field only.²⁷ However, a different behavior was observed in the thalamus, where no between-group difference in

TABLE 3. R_2 relaxivity slopes $S = (1/T_2^{(3T)} - 1/T_2^{(1.5T)}) / \Delta B$ [$s^{-1}T^{-1}$], Where ΔB Is a Difference in Magnetic Fields

R_2 slope	GP	Put	CN	Th
Neuro-WD	2.07 (0.53)	1.53 (0.50)	1.23 (0.50)	0.55 (0.26)
Hep-WD	1.62 (0.69)	1.01 (0.34)**	0.95 (0.41)	0.30 (0.12)***
Controls	1.52 (0.31)***	1.09 (0.28)***	0.85 (0.23)**	0.26 (0.15)***

The slope is listed for following structures: globus pallidus (GP), putamen (Put), caudate nucleus (CN), and thalamus (Th). Standard deviations are in parentheses.

* $P < 0.05$.

** $P < 0.01$, and.

*** $P < 0.001$ for the post-hoc between-group analysis of control and hep-WD vs. neuro-WD group.

T_2 was found at 3T, while the R_2 relaxivity slope was steeper in the neuro-WD group compared to controls. The explanation of these disparate results is unclear. We hypothesize that R_2 field dependence in this case is not driven by iron concentration alone, but rather by pathological tissue changes prolonging T_2 relaxation time, such as demyelination or increased free water content, which contribute to relaxivity at 1.5T to a disproportionately higher degree than at 3.0T.

In contrast to previous brain MRI studies of untreated hepatic WD patients, we observed no significant changes in quantitative MR parameters in our long-term-treated hep-WD patients.^{2,28} We can hypothesize that, unlike in neurological WD patients, abnormalities visible on brain MRI in hepatic WD patients may be reversible with appropriate treatment. This theory, however, needs to be confirmed by a longitudinal study with a larger number of subjects.

Several limitations of this study have to be mentioned. First, due to scanning time restrictions, we did not use other quantitative techniques, namely DTI, which could bring further information on the WD neuropathology. Additionally, a small number of patients were examined, particularly in the hep-WD group, which is composed only of patients with mild symptoms. Therefore, the conclusions about hep-WD patients must be generalized only with caution.

In conclusion, using multiparametric mapping we observed significant residual brain tissue abnormalities in neurological WD patients on chronic anticopper treatment. However, no such changes were found in treated patients with the hepatic form of WD. Higher magnetic susceptibility observed in DGM in neuro-WD patients was corroborated by decreased T_2 and T_2^* relaxation times in GP, Put, and CN, which we attribute to increased iron content (probably in the form of hemosiderin deposits). The results of quantitative MR metrics in the thalamus suggest a scenario of demyelination in the neuro-WD group.

References

1. Czlonkowska A, Litwin T, Dusek P, et al. Wilson disease. *Nat Rev Dis Primers* 2018;4:21.
2. Litwin T, Gromadzka G, Czlonkowska A, Golebiowski M, Poniatowska R. The effect of gender on brain MRI pathology in Wilson's disease. *Metab Brain Dis* 2013;28:69–75.
3. Zhong W, Huang Z, Tang X. A study of brain MRI characteristics and clinical features in 76 cases of Wilson's disease. *J Clin Neurosci* 2019; 59:167–174.
4. Kozic DB, Petrovic I, Svetel M, Pekmezovic T, Ragaji A, Kostic VS. Reversible lesions in the brain parenchyma in Wilson's disease confirmed by magnetic resonance imaging: Earlier administration of chelating therapy can reduce the damage to the brain. *Neural Regen Res* 2014;9:1912–1916.
5. Sinha S, Taly AB, Prashanth LK, Ravishankar S, Arunodaya GR, Vasudev MK. Sequential MRI changes in Wilson's disease with de-coppering therapy: A study of 50 patients. *Br J Radiol* 2007;80:744–749.
6. Dusek P, Litwin T, Czlonkowska A. Neurologic impairment in Wilson disease. *Ann Transl Med* 2019;7(Suppl 2):S64.
7. Skowronska M, Litwin T, Dziezyc K, Wierzchowska A, Czlonkowska A. Does brain degeneration in Wilson disease involve not only copper but also iron accumulation? *Neurol Neurochir Pol* 2013;47:542–546.
8. Dusek P, Bahn E, Litwin T, et al. Brain iron accumulation in Wilson disease: A post mortem 7 Tesla MRI — Histopathological study. *Neuropathol Appl Neurobiol* 2016;43:514–532.
9. Fritsch D, Reiss-Zimmermann M, Trampel R, Turner R, Hoffmann KT, Schafer A. Seven-Tesla magnetic resonance imaging in Wilson disease using quantitative susceptibility mapping for measurement of copper accumulation. *Invest Radiol* 2014;49:299–306.
10. Dusek P, Skoloudik D, Maskova J, et al. Brain iron accumulation in Wilson's disease: A longitudinal imaging case study during anticopper treatment using 7.0T MRI and transcranial sonography. *J Magn Reson Imaging* 2018;47:282–285.
11. Bartzokis G, Aravagiri M, Oldendorf WH, Mintz J, Marder SR. Field dependent transverse relaxation rate increase may be a specific measure of tissue iron stores. *Magn Reson Med* 1993;29:459–464.
12. Dezortova M, Herynek V, Krssak M, Kronerwetter C, Trattnig S, Hajek M. Two forms of iron as an intrinsic contrast agent in the basal ganglia of PKAN patients. *Contrast Media Mol Imaging* 2012;7:509–515.
13. Parker DL, Payne A, Todd N, Hadley JR. Phase reconstruction from multiple coil data using a virtual reference coil. *Magn Reson Med* 2014; 72:563–569.
14. Acosta-Cabronero J, Cardenas-Blanco A, Betts MJ, et al. The whole-brain pattern of magnetic susceptibility perturbations in Parkinson's disease. *Brain* 2017;140:118–131.
15. Schofield MA, Zhu Y. Fast phase unwrapping algorithm for interferometric applications. *Opt Lett* 2003;28:1194–1196.
16. Li W, Wu B, Liu CL. Quantitative susceptibility mapping of human brain reflects spatial variation in tissue composition. *Neuroimage* 2011;55: 1645–1656.
17. Liu T, Wiesnieff C, Lou M, et al. Nonlinear formulation of the magnetic field to source relationship for robust quantitative susceptibility mapping. *Magn Reson Med* 2013;69:467–476.
18. Herynek V, Wagnerova D, Hejlova I, Dezortova M, Hajek M. Changes in the brain during long-term follow-up after liver transplantation. *J Magn Reson Imaging* 2012;35:1332–1337.
19. Marquardt D. An algorithm for least squares estimation of non-linear parameters. *J Soc Ind Appl Math* 1963;11:431–434.
20. R Core Team. *R: A language and environment for statistical computing*. R Foundation for Statistical Computing, Vienna, Austria. 2018. URL <https://www.R-project.org/>.
21. Langkammer C, Krebs N, Goessler W, et al. Quantitative MR imaging of brain iron: A postmortem validation study. *Radiology* 2010;257:455–462.
22. Hallgren B, Sourander P. The effect of age on the non-haemin iron in the human brain. *J Neurochem* 1958;3:41–51.
23. Vymazal J, Zak O, Bulte JW, Aisen P, Brooks RA. T1 and T2 of ferritin solutions: Effect of loading factor. *Magn Reson Med* 1996;36:61–65.
24. Gossuin Y, Muller RN, Gillis P. Relaxation induced by ferritin: A better understanding for an improved MRI iron quantification. *NMR Biomed* 2004;17:427–432.
25. Li G, Zhou X, Xu P, Pan X, Chen Y. Microstructure assessment of the thalamus in Wilson's disease using diffusion tensor imaging. *Clin Radiol* 2014;69:294–298.
26. Van Wassenae-van Hall HN. Neuroimaging in Wilson disease. *Metab Brain Dis* 1997;12:1–19.
27. Uddin MN, Lebel RM, Wilman AH. Value of transverse relaxometry difference methods for iron in human brain. *Magn Reson Imaging* 2016;34:51–59.
28. Kozic D, Svetel M, Petrovic B, Dragasevic N, Semnic R, Kostic VS. MR imaging of the brain in patients with hepatic form of Wilson's disease. *Eur J Neurol* 2003;10:587–592.